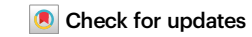


https://doi.org/10.1038/s41467-025-62027-y

Requirements for next-generation integrated photonic FMCW LiDAR sources

Simone Bianconi, Pol Ribes-Pleguezuelo & Fabrizio Silvestri



We introduce a framework for the design of photonic integrated laser sources for FMCW LiDAR, evaluating trade-offs in key laser metrics such as linewidth, chirp linearity and rate, based on laser-system co-design metrics. We review the main performance requirements for midrange applications, with the goal of guiding ongoing research and commercial development.

Frequency-modulated continuous-wave (FMCW) LiDAR offers significant advantages over direct time-of-flight (ToF) LiDAR systems, including enhanced resistance to external interference, superior range resolution, and the ability to detect object velocity by directly measuring the Doppler shift. These characteristics make FMCW LiDAR particularly well-suited for applications requiring high precision and robustness, such as autonomous vehicles, robotics, remote sensing, and industrial metrology. Its capability to operate in challenging environments with reduced susceptibility to ambient light and multipath interference further extends its appeal to aerospace, defense, and advanced manufacturing sectors. In addition, Doppler-based velocity measurement provides instantaneous and direct velocity data for each point in the scene, which is advantageous in autonomous applications to enhance safety, decision-making, and real-time control, as well as in specific aerospace applications that demand direct high-speed measurements, such as rover landing and space debris avoidance and removal.

Implementing an FMCW LiDAR system presents several technological challenges, particularly regarding the laser source, which plays a critical role in determining the system's performance as well as its cost and size. The laser must exhibit low phase noise and high coherence in order to achieve high range resolution and minimize signal degradation. Additionally, highly linear frequency chirping is required to ensure accurate distance measurements, typically demanding advanced modulation or linearization techniques and feedback control mechanisms. Maintaining a balance between tuning range and phase noise while optimizing for wavelength selection remains a key challenge in the development of practical and high-performance FMCW LiDAR systems.

Integrated photonics offers a promising solution to many of the challenges associated with FMCW LiDAR by providing compact, stable, and scalable laser sources with unmatched performance characteristics. Monolithic integration of photonic integrated circuits (PIC) enables precise control over chirp linearity and phase noise, addressing two of the most critical factors for high-resolution ranging and velocity measurement. Furthermore, integrated photonic platforms facilitate the on-chip integration of photonic components for

modulation, stabilization, and beam steering, reducing the need for bulky external components while enhancing reliability and manufacturability. Finally, the potential for large-scale wafer-level production also supports cost reduction, making high-performance FMCW LiDAR systems more accessible for applications such as autonomous driving, industrial automation, and remote sensing.

Despite their advantages, integrated photonic laser sources for FMCW LiDAR still face several limitations that must be addressed for widespread adoption. Power output and efficiency are some of the main constraints, as integrated photonic lasers typically provide lower output power than bulk legacy sources, often requiring external optical amplification. Furthermore, the hybrid integration of active and passive components, such as semiconductor gain sections with PIC, presents fabrication and packaging challenges that impact yield and scalability, currently limiting the technology readiness level (TRL) of these systems. Finally, the constant drive for performance improvement of photonic integrated lasers in terms of noise and tuning characteristics should be guided by design principles based on system-level considerations in order to effectively benefit FMCW LiDAR applications.

In this commentary, we introduce a simple theoretical framework for evaluating performance trade-offs in PIC-based FMCW sources, such as chirp linearity versus linewidth, validated against recent laser designs. We also propose a deployment road-map for mid-range autonomous and aerospace applications, based on laser-system codesign metrics. These design principles are intended to provide guidance for the design and implementation of photonic integrated lasers for FMCW LiDAR. Researchers and technologists can use the models summarized in this commentary to estimate the range resolution and refresh rates of a related LiDAR instrument and compare them against the performance requirements of the envisioned application to better focus development efforts to the area of major benefit for system performance.

FMCW metrics

FMCW LiDAR operates by transmitting a laser signal with a continuously varying frequency (chirp) and measuring the coherent beat frequency between the signal received after reflection from a target and a local oscillator (LO). The time delay is encoded into the detected frequency shift, providing range information, while the target's velocity can be simultaneously extracted from the Doppler shift. The most common implementation of this LiDAR scheme entails a triangular chirp, as shown in Fig. 1a: the generated beat notes from the ascending and descending ramps enable to simultaneously retrieve the range and velocity information.

Laser linewidth and chirp linearity. Since the range information is encoded in the detected beat note, as shown in Fig. 1a, the range resolution is therefore determined by the spectral linewidth of this

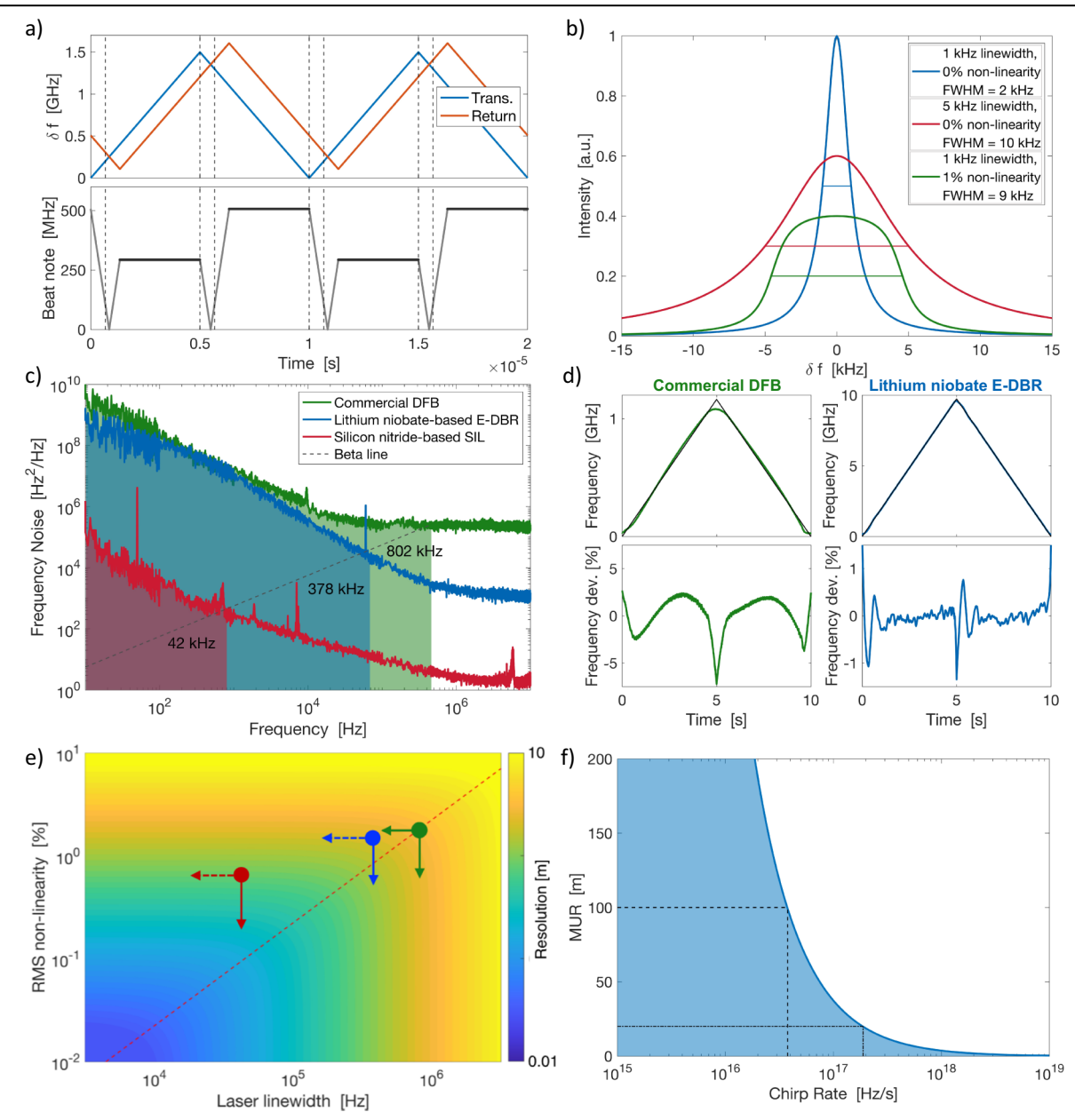


Fig. 1 | **The effect of photonic integrated laser characteristics on FMCW LiDAR performance. a** Conceptual schematic of FMCW LiDAR for a triangular chirp scheme. The return signal is delayed in time and shifted by the Doppler effect, resulting in two distinct beat notes detected in a chirp period, simultaneously encoding the range and velocity information. **b** Simulated spectral distribution and linewidth of the detected beat note for different laser source characteristics (linewidth and chirp linearity), assuming a 100-m target range, 1-ms chirp period, and 150 MHz chirp range. The thinner horizontal lines indicate the full width at half maximum (FWHM) of each detected beat note, whose value is also reported in the legend. **c** Measured frequency noise spectra for three state-of-the-art laser sources for FMCW LiDAR: a commercial DFB laser, an external cavity photonic integrated laser based on extended distributed Bragg reflector (E-DBR) in lithium niobate⁸, and a tunable self-injection locked photonic integrated laser based on silicon nitride⁵. **d** Chirp non-linearity measured for the first two lasers analyzed in panel c): the top panels show the frequency chirp measured using an imbalanced

Mach-Zehnder interferometer (MZI), while the bottom panel shows the extracted deviation from an ideal linear chirp. **e** Simulated FMCW LiDAR range resolution as a function of laser linewidth and chirp linearity, assuming a 30-m target range, 100-ms chirp period, and 5-GHz chirp range. The same three lasers as in (**c**) are also included in this analysis, with their characteristics represented by color-coded dots on the performance map: the arrows represent technological improvements in laser linewidth (horizontal arrows) or chirp linearity (vertical arrow), with the solid arrow showing the preferred direction for best performance improvement, and the dashed arrow the direction with only marginal improvement. **f** Maximum unambiguous range (MUR) as a function of chirp rate, assuming a detector bandwidth of 25 GHz: the blue shaded area represents the ranges that can be targeted with a given chirp rate (i.e., resulting in a maximum detected beat note lower than the limit of 25 GHz). The same color coding was used in panels (**c**-**e**) to represent the three laser sources analyzed.

beat note. For an ideal laser transmitter, the range resolution is ultimately limited by the speed of light c and the total chirp range B, as $\delta R = c/2B^2$. In non-ideal scenarios, however, the range resolution is also affected by two key parameters of the laser source: the phase noise of the laser and the chirp linearity. In the example proposed in Fig. 1b, a 1% non-linearity of the chirp (defined as the normalized RMS deviation from the linear chirp) has the same detrimental effect on the range resolution as a fivefold increase in laser linewidth.

Integrated photonics can offer unique advantages on both these fronts. On the one hand, the extremely high quality factor resonators demonstrated in integrated photonic platforms enable the implementation of compact external cavity lasers (ECL) reaching phase noise levels well below those of state-of-the-art lasers³, as showcased in Fig. 1c. On the other hand, these laser architectures can leverage the monolithic integration of frequency-tuning element to achieve fast and highly linear tuning by maximizing the actuation efficiency and bandwidth while minimizing the coupling to external mechanical and electrical noise sources⁴. As an example, Fig. 1d shows the chirp linearity of a photonic integrated ECL based on lithium niobate compared to that of a state-of-the-art commercial DFB laser.

In order to effectively guide the ongoing research and advancements in photonic integrated laser technology and to ensure that trade-offs between improving laser phase noise and chirp linearity are carefully evaluated⁵, a well-directed development approach is essential.

The range resolution formula discussed above can be modified to account for the effects of laser linewidth and chirp linearity (see Supplementary Information). Assuming a quadratic non-linearity, the depth resolution can be expressed as:

$$\delta R = c\sqrt{\left(\sqrt{5}\tau(2\tau/T - 1)\sigma_{RMS}\right)^2 + \left(\gamma/\beta\right)^2}$$
 (1)

where τ is the round-trip delay, T and β are the chirp period and rate, σ_{RMS} is the RMS chirp non-linearity and γ' is the averaged laser linewidth.

Figure 1e showcases an example of the combined effect of laser linewidth and chirp linearity on the range resolution of a 100-m ranging FMCW LiDAR instrument with a 1-ms repetition period, obtained using the model derived in the Supplementary Information. As validation of the model presented in equation (1), we included in this performance map the three laser sources analyzed in Fig. 1c, d, summarized in Table 1, and represented by the three colored dots in Fig. 1e.

This performance estimation underscores the importance of a well-guided development effort. For instance, the ultra-narrow-linewidth self-injection locked laser⁵ (represented by the red dot in Fig. 1e), would see limited gains in range resolution from a further reduction in phase noise. In contrast, an improvement in its chirp linearity can be highly beneficial to its performance.

Table 1 | Key performance metrics of commercial and PIC-based lasers used in the range resolution performance estimation in Fig. 1e

Laser architecture	Material	Linewidth (1 ms)	Non-linearity
DFB	InP/InGaAs	802 kHz	1.8%
E-DBR	Lithium niobate	378 kHz	1.5%
SIL	Silicon nitride	42 kHz	0.65%

DFB distributed feedback laser, E-DBR extended distributed Bragg reflector laser, SIL self-injection locked laser.

Ambiguity range and chirp rate. The monolithic integration of frequency-tuning elements in integrated photonic lasers enables extremely fast and wide wavelength tuning capabilities, with recent demonstrations of chirp rates reaching the exa-hertz-per-second⁶⁻⁸. While of interest for applications requiring fast switching of the laser wavelength, these extremely high chirp rates are of limited benefit to most FMCW LiDAR applications. In fact, despite facilitating fast signal acquisition and broad tuning range, they offer no improvement to the range resolution. This is because of the range ambiguity that occurs when the round-trip delay is greater than the chirp repetition rate. The chirp repetition period T is therefore limited by the maximum unambiguous range (MUR), which is given by MUR = cT/4 for a triangular chirped FMCW LiDAR. The highest beat note frequency that the system must be able to measure is therefore set by the chirp rate β as $f_{\text{max}} = \beta T/2$. In most FMCW LiDAR applications, this frequency is limited to a few tens of gigahertz at most, in order to limit the cost, size, and complexity of the required detectors and acquisition electronics. As a result of this limitation, Fig. 1f shows the highest useful chirp rate as a function of MUR, assuming a detector bandwidth of 25 GHz: it is evident that chirp rates exceeding 10¹⁷ Hz/s are only useful for very short-range FMCW LiDAR applications.

Output power and signal-to-noise ratio. Transmitted power is a fundamental parameter in FMCW LiDAR, as it directly influences both the signal-to-noise ratio (SNR) and carrier-to-noise ratio (CNR), as described by the LiDAR equations^{9,10}. The development of photonic integrated lasers with high output power remains a significant challenge due to the constraints imposed by their integrated architecture, such as optical coupling losses and complicated thermal management, as well as to the low maturity of hybrid assembly technologies.

Off-chip amplification of highly coherent laser sources has enabled FMCW ranging over distances of few kilometers¹¹. However, the corresponding increase in complexity, size, weight, and power (SWaP) may diminish the appeal of a fully photonic integrated solution. For this reason, increasing efforts have been devoted to the monolithic integration of III-V gain media on photonic integrated circuits, both for high-power lasers and for on-chip amplification^{12–14}. In addition, the advent of novel hybrid integration technologies such as photonic wire bonding¹⁵ is one of the most promising avenues for improving the power output of photonic integrated lasers¹⁶.

Incidentally, received power and signal-to-noise ratio are additional factors limiting the repetition rate used in realistic FMCW scenarios. This is because in continuous-wave techniques such as FMCW, the number of transmitted and return photons is directly proportional to the duration of the repetition period (for a fixed CW output power). Similar to the case of range ambiguity discussed above, this in turn results in limiting the range of maximum useful chirp rates.

Application requirements

FMCW technology has attracted increasing interest across a variety of sectors, ranging from robotics to security and agriculture¹⁷. Here we will primarily focus on the requirements for the major application cases for mid-range FMCW LiDAR: terrestrial automation and aerospace sensors.

Terrestrial applications. FMCW LiDAR holds significant promise for terrestrial mid-and long-range applications, including for automotive, advanced robotics, industrial automation, and infrastructure monitoring. In particular, this technology has garnered considerable

attention from the automotive industry thanks to its inherent background noise rejection, a key advantage of coherent detection that ensures robust sensor operation across multiple independent vehicles. In addition, Doppler velocity measurement enabled by FMCW LiDAR is highly valuable for automation because it enables direct, real-time detection of relative motion, allowing for faster and more accurate decision-making than relying solely on positional changes between successive frames. Finally, low-SWaP FMCW LiDAR instruments deployed on the ground or onboard autonomous airborne platforms (e.g., drones or balloons) can find application in earth science, for topographical measurements such as tree canopy mapping, rock morphometry, and structural monitoring.

This interest has further intensified with the advent of integrated photonics, which promises compact FMCW instruments that can not only be manufactured at scale, but can also monolithically integrate additional instrument functionalities such as non-mechanical beam steering optics and coherent receivers on the same platform¹⁷⁻²⁰. In recent years, a plethora of PIC-based FMCW LiDAR instrument concepts have been demonstrated^{17,21}, ranging from scanning systems²²⁻²⁵ to integrated multi-channel receivers²⁶⁻²⁸ and AI-enabled multi-sensor fusion^{29,30}.

Typical requirements for automation entail measurement range up to 300-m ranges, cm-scale resolution, and ~0.1° angular resolution³¹. In addition, automotive applications typically require the ability to measure relative velocity up to 140 km/h at a distance of 200 m, with a frame refresh rate of 30 Hz³². In many applications, such as automotive, finally, these requirements are accompanied by eye safety and refresh rate constraints, which lead to a set of system tradeoffs which characterize the main current research challenges for PIC-based FMCW LiDAR:

- · Eye safety operation vs achievable range
- · Field of view & lateral resolution vs refresh rate
- · Doppler velocity vs speed of digital readout
- · Point rate vs computational workload

Some of these trade-offs can be quantitatively assessed by using a modified form of the LiDAR equation for carrier-to-noise ratio³³:

$$CNR = \frac{P_{tr}}{E_{ph}} \frac{\rho \, \eta}{F \, N_H N_V} \frac{A_R}{\pi R^2} \tag{2}$$

where P_{tr} is the average transmitter power, E_{ph} is Photon's energy, F is the frame rate, ρ the reflectivity of the target, N_H , N_V are respectively the number of scene points in the horizontal (H) and vertical (V) direction, A_R is the area of the receiving optics, R is the range, and η an overall efficiency accounting for system transmission and channel effects (atmospheric attenuation, speckle effects).

As demonstrated by equation (2), achieving higher resolution or faster scene refresh rate requires a corresponding increase in received optical power. This requirement becomes even more pronounced when extending the maximum range, which demands a quadratic increase in optical power. This additional power can only be supplied through optical amplification—although ultimately constrained by eye safety regulations—or by employing a larger aperture optical system, hence increasing the overall mass and volume of the instrument. As a result, the maximum attainable resolution, range, and refresh rate for a given application scenario are fundamentally constrained, regardless of the specific FMCW LiDAR architecture. This limitation also applies to integrated FMCW receivers featuring arrays of optical channels

enabled, for example, by optical phased arrays (OPA)³⁴, as discussed in more detail in the Supplementary Information. The constraint holds true irrespective of whether the channel arrays are implemented in the transmission or receiver side, and whether a point-scanning, line-scanning, or flood illumination technique is employed.

Ultimately, the feasibility of a given design is dictated by the net energy balance in a specific application scenario, which remains independent of the specific detection and scanning scheme used. The primary challenge in achieving an effective PIC-based FMCW LiDAR implementation is increasing output power and enhancing optical collection efficiency, which would enable longer-range operation as well as faster scene refresh rates.

Aerospace. The unique ability of photonic integrated FMCW instruments to provide a combined measurement of the range and speed of targets within a low-SWaP platform has attracted increasing interest in the aerospace sector, for applications such as debris removal, rendezvous, and docking for in-orbit servicing³⁵.

Due to the limited output power of photonic integrated FMCW sources, their use cases are constrained to maximum ranges of a few hundreds of meters, namely:

- altimetry (≤1 km)
- rendezvous and docking—including for in-orbit servicing or space debris removal
- landing
- · rover navigation
- shape monitoring of large deployable antennas and telescopes

Doppler velocity measurement is sought after in applications such as spacecraft landing, in-orbit servicing, debris removal, and vibration monitoring, where instantaneous velocity information is critical for safe maneuvering, fine control, and dynamic response in space environments where traditional inertial or optical methods may be limited. In these contexts, even more advanced scientific measurements, such as wind and dust speed and exhaust plume mapping, could become feasible as the performance of integrated photonic FMCW LiDAR improves over the next years. Table 2 presents the approximate generic requirements for the main FMCW LiDAR applications mentioned above.

The interesting overlap of these ranging requirements with those of the automotive sector indicates a potential synergy between the two application fields, which can help propel the maturity of photonic integrated FMCW technology. As an example, an FMCW LiDAR instrument for lunar descent payload, with a field of view (FoV) of 25×25 degrees, with a maximum measurement range of 1 km and a point accuracy of 5.8 mm at 500 m, was demonstrated using a combination of a fiber laser with a PIC-based receiver array, such as those developed in the automotive sector³⁵.

The TRL for most integrated photonic FMCW LiDAR for aerospace applications is currently at the early demonstrator phase (TRL4 to TRL5). Several prototypes demonstrated satisfactory ranging performance in line with the above-mentioned requirements of the automotive and aerospace sectors, but only a few started the de-risking of critical functions or the qualification of components for real use case scenarios. PIC-based instruments are yet to demonstrate their robustness against vibrations, shock, and radiation. The stability of the optical path and thermal load management are also crucial for the deployment onboard autonomous platforms for the aerospace application mentioned above.

Table 2 | Approximate typical requirements for mid-range FMCW LiDAR space applications; specific values depend on mission and scenario

Application	Range	Resolution	Velocity	Mass	FoV
Rendezvous and docking—in-orbit servicing—space debris removal	0-2000 m	1 cm	2-50 cm/s	~1.33 kg	≥10°
Landing	10-3000 m	≤30 cm	~30 m/s	≤5 kg	≥10°
Rover navigation	1–100 m	1 cm	1 m/s	≤1 kg	≥80°
Antenna and telescope shape monitoring	≤20 m	~10 µm	N.A.	~1.33 kg	depends on mission

When a range is specified, it is intended to report typical minimum and maximum values. Here, we omitted the altimetry use case, for which commercial off-the-shelf (COTS) ranging instruments already offer km-range instruments within compact enough platforms (<1 kg)³⁶.

Market and economic considerations

FMCW LiDAR systems based on integrated photonics hold significant promise for large-scale deployment, particularly by enabling mass production through established microelectronics fabrication techniques, which can drastically reduce per-unit costs. This is especially appealing for automotive applications, where cost and scalability are key drivers. The resulting reduction in costs would largely benefit the deployment of PIC-based FMCW LiDAR in other, more niche applications and markets. Nonetheless, the photonic packaging of massmanufactured PIC components can still drive considerable per-unit cost, encouraging the development of simple architectures with minimal reliance on delicate optical interfaces such as fiber coupling or individual hybrid integration with semiconductor gain chips, in order to maximize robustness and manufacturability at scale.

Another important consideration on the price and mass-scale deployment of photonic integrated FMCW LiDAR systems is their intrinsic complexity and reliance on intense data processing. The sophisticated control and acquisition electronics required can significantly contribute to the total cost and power consumption of the overall instrument, especially when targeting very low per-unit cost for mass-scale deployment.

In contrast, for space and aerospace applications, cost is often a secondary concern compared to the ability to minimize payload mass and volume, given the inherently high expenses associated with launching and operating equipment in such environments. In these contexts, the substantial reduction in size and weight offered by PIC-based LiDAR can be far more critical, potentially justifying a higher cost.

Prospects and challenges

In this commentary, we introduced a framework for guiding future research and development efforts in lasers for FMCW LiDAR based on laser-system co-design metrics. The models and analyses highlight areas of focus for technological development and common performance trade-offs. Most notably, the combined effect of laser linewidth and chirp linearity on the FMCW LiDAR range resolution implies that some recently reported photonic integrated lasers can benefit significantly more from improving the chirp linearity rather than the laser linewidth, or vice versa. Similarly, the analysis revealed that the chirp rates achieved in recently reported photonic integrated lasers are more than sufficient for the needs of most FMCW LiDAR systems.

Moreover, a review of the main performance requirements for mid-range autonomous and aerospace applications, reveals that future research and development efforts in photonic integrated lasers for FMCW LiDAR should focus on output power and robust co-packaging of the photonic and electronic components, able to handle the stringent environmental requirements, while still maintaining a low SWaP. The integration of complementary technologies, such as free-form optical design, can allow for extending the maximum range or resolution by incorporating large collecting apertures for better optical collection efficiency. While PIC integration can enable a reduction in system SWaP, the need for a large collecting aperture and computationally intensive architectures may offset these gains, making the success of PIC-based FMCW LiDAR dependent on advancements not only in photonics and optical design, but also in electronics, firmware, and their seamless integration.

Simone Bianconi ®¹ ⊠, Pol Ribes-Pleguezuelo ®² & Fabrizio Silvestri ®³

¹Swiss Federal Institute of Technology Lausanne (EPFL), Lausanne 1015, Switzerland. ²ESA, ESTEC, Keplerlaan 1, Noordwijk NL-2200, The Netherlands. ³High Tech Industry Unit, TNO, Stieltjesweg 1, Delft 2628 CK. The Netherlands. ⊠e-mail: simone.bianconi@epfl.ch

Received: 28 February 2025; Accepted: 9 July 2025;

References

Published online: 22 July 2025

- Riemensberger, J. et al. Massively parallel coherent laser ranging using a soliton microcomb. Nature 581, 164-170 (2020).
- 2. Richards, M. A. Fundamentals of Radar Signal Processing (McGraw-Hill Professional, 2005).
- Li, B. et al. Reaching fiber-laser coherence in integrated photonics. Opt. Lett. 46, 5201–5204 (2021).
- Siddharth, A. et al. Piezoelectrically tunable, narrow linewidth photonic integrated extended-dbr lasers. Optica 11, 1062-1069 (2024).
- Voloshin, A. et al. Monolithic piezoelectrically tunable hybrid integrated laser with sub-fiber laser coherence. Optica 12, 8 (2025).
 Snigirev, V. et al. Ultrafast tunable lasers using lithium niobate integrated photonics. Nature
- 615, 411-417 (2023).7. Xue, S. et al. Pockels laser directly driving ultrafast optical metrology. Light Sci. Appl. 14,
- Xue, S. et al. Pockels laser directly driving ultrafast optical metrology. Light Sci. Appl. 14, 209 (2025).
- Siddharth, A. et al. Ultrafast tunable photonic-integrated extended-dbr pockels laser. Nat. Photonics 19, 709–717 (2025).
- Barber, Z. W., Dahl, J. R., Sharpe, T. L. & Erkmen, B. I. Shot noise statistics and information theory of sensitivity limits in frequency-modulated continuous-wave ladar. J. Opt. Soc. Am. A 30, 1335–1341 (2013).
- Gatt, P. & Henderson, S. W. Laser radar detection statistics: a comparison of coherent and direct-detection receivers. Proc. SPIE 4377, 251–262 (2001).
- Feneyrou, P., Martin, A., Dolfi, D. & Payot, E. 3d imaging with large range dynamics and simultaneous accurate speed measurement. Appl. Opt. 63, 5387–5394 (2024).
- Avraam, C., Sousa, T., Mckenzie, I., Armandillo, E. & Iezekiel, S. in Space-based Lidar Remote Sensing Techniques and Emerging Technologies. LIDAR 2023 (Springer, 2024).
- Pérez-Serrano, A., Quevedo-Galán, C., Aguilera-Sánchez, V. R., Tijero, J. M. G. & Esquivias, I. Differential absorption lidar transmitter based on an indium phosphide photonic integrated circuit for carbon dioxide sensing. *IEEE J. Sel. Top. Quantum Electron.* 28, 1-8 (2022).
- Xiang, C. et al. High-performance silicon photonics using heterogeneous integration. IEEE J. Sel. Top. Quantum Electron. 28, 1-15 (2021).
- Franken, C. A. et al. High-power and narrow-linewidth laser on thin-film lithium niobate enabled by photonic wire bonding. APL Photonics 10, 026107 (2025).

- Sherman, J. et al. In Space-based Lidar Remote Sensing Techniques and Emerging Technologies (Springer, 2024).
- 17. Bogue, R. The growing importance of lidar technology. Ind. Robot 49, 1025-1031 (2022).
- 18. Chen, R. et al. Integrated adaptive coherent lidar for 4d bionic vision. Preprint at arXiv:2410.08554 (2024).
- 19. Kuse1, K. & Fermann, M. E. Frequency-modulated comb lidar. APL Photon. 4, 106105 (2019).
- Li, B., Lin, Q. & Li, M. Frequency-angular resolving lidar using chip-scale acousto-optic beam steering. Nature 620, 316–322 (2023).
- Aurora. https://blog.aurora.tech/engineering/fmcw-lidar-the-self-driving-gamechanger (2024).
- Photonics, S. Scantinel technology overview- white paper. https://www.scantinel.com (2022).
- 23. SiLCs. https://www.silc.com/home/ (2024).
- Rogers, C. et al. A universal 3d imaging sensor on a silicon photonics platform. Nature 590, 256–261 (2021).
- 25. Aeva, A. https://www.aeva.com/atlas/ (2025).
- Martin, A. et al. Photonic integrated circuit-based fmcw coherent lidar. J. Lightwave Technol. 36, 4640–4645 (2018).
- Royo, S. & Ballesta-Garcia., M. An overview of lidar imaging systems for autonomous vehicles. MDPI Appl. Sci. 9, 4093 (2019).
- 28. Ommatidia. https://ommatidia-lidar.com/ (2024).
- Continental. https://www.continental.com/en/press/press-releases/20210714-lidar-aeve/ (2025).
- mobileye. https://static.mobileye.com/website/corporate/media/radar-lidar-fact-sheet. pdf (2024).
- Wu, Z. et al. Advancements in key parameters of frequency-modulated continuous-wave light detection and ranging: a research review. Appl. Sci. 14, 7810 (2024).
- 32. Dai, Z. et al. Requirements for automotive lidar systems. Sensors 22, 7532 (2022).
- 33. McManamon, P. Field Guide to LiDAR (SPIE, 2015).
- Hsu, C.-P. et al. A review and perspective on optical phased array for automotive lidar. IEEE J. Sel. Top. Quantum Electron. 27, 1-16 (2020).
- Margallo, E. et al. Space-based Lidar Remote Sensing Techniques and Emerging Technologies (Springer, 2024).
- 36. Jenoptik. https://www.jenoptik.com/products/lasers/laser-distance-sensors/dlem (2024).

Acknowledgements

The authors thank Dr. Andrey Voloshin for insightful discussions on laser technology and FMCW requirements.

Author contributions

S.B. developed the modeling of the effects of laser characteristics on FMCW LiDAR performance and analysis of state-of-the-art photonic integrated lasers. P.R.-P. and F.S. performed the analysis of application-specific requirements for terrestrial and aerospace applications. All authors discussed the findings and wrote the manuscript.

Competing interests

The authors declare no competing interests.

Additional information

Supplementary information The online version contains supplementary material available at https://doi.org/10.1038/s41467-025-62027-y.

Correspondence and requests for materials should be addressed to Simone Bianconi.

Peer review information *Nature Communications* thanks Grégory Pandraud and Michael Zanetti for their contribution to the peer review of this work.

Reprints and permissions information is available at

http://www.nature.com/reprints

Publisher's note Springer Nature remains neutral with regard to jurisdictional claims in published maps and institutional affiliations.

Open Access This article is licensed under a Creative Commons Attribution-NonCommercial-NoDerivatives 4.0 International License, which permits any non-commercial use, sharing, distribution and reproduction in any medium or format, as long as you give appropriate credit to the original author(s) and the source, provide a link to the Creative Commons licence, and indicate if you modified the licensed material. You do not have permission under this licence to share adapted material derived from this article or parts of it. The images or other third party material in this article are included in the article's Creative Commons licence, unless indicated otherwise in a credit line to the material. If material is not included in the article's Creative Commons licence and your intended use is not permitted by statutory regulation or exceeds the permitted use, you will need to obtain permission directly from the copyright holder. To view a copy of this licence, visit http://creativecommons.org/licenses/by-nc-nd/4.0/.

© The Author(s) 2025